Photophysical Properties and Energy Transfer Pathway of Er(III) Complexes with Pt−Porphyrin and Terpyridine Ligands

Min-Kook Nah,[†,‡] Jae Buem Oh,[†] Hwan Kyu Kim,*[,†,#] Kyong-Hoon Choi,[§] Yong-Rok Kim,[§] and Jun-Gill Kang*[,‡]

Center for Smart Light-Harvesting Materials and Department of Advanced Materials, Hannam University, Deajeon 306-791, Korea, Department of Chemistry, Yonsei University, Seoul 120-749, Korea, and Department of Chemistry, Chungnam National University, Daejeon 304-764, Korea

Received: December 22, 2006; In Final Form: April 16, 2007

The photophysical properties of Er(III) complexes coordinated with platinum[5,10,15-triphenyl-20-(4-carboxyphenyl)-porphyrin] (PtP) and terpyridine (tpy) ligands in organic solution were investigated. The Er(III) complex emitted sensitized near-IR (NIR) luminescence when the PtP ligands were excited under deoxygenated conditions. The quantum yield (Φ_{Ln}) of the sensitized luminescence was 0.015%, as evaluated from luminescence lifetime. The photophysical studies and theoretical calculations suggest that the Förster resonance mechanism is very suitable for the energy transfer from PtP to the Er(III) ion and occurred through the first triplet excited state of PtP. The 12.3% energy transfer from the triplet state to the $^4F_{9/2}$ and $^4I_{9/2}$ states of Er(III) occurred with a rate distribution of 3.36×10^5 and 6.67×10^4 s^{-1}, respectively. In addition, the observed triplet quantum yield of the PtP ligand in [Ln(PtP)$_3$(tpy)] proved that the energy transfer from the singlet excited state of the PtP ligand to the Er(III) ion did not take place.

Introduction

The intriguing luminescence properties of several lanthanide complexes are well documented and include hypersensitivity to the coordination environment, narrow luminescence bandwidth, and relatively long luminescence lifetime.[1] The near infrared (NIR) luminescence emitted by lanthanide ions of Yb(III), Nd(III), and Er(III) has many practical applications, particularly in optical communications. These ions have characteristic luminescence at wavelengths close to 980, 1300, and 1500 nm, which are required for optical communication. However, their absorption cross sections are intrinsically low owing to partially allowed f → f transitions. For instance, high concentrations of Er(III) ions can emit undesirable luminescence by other photophysical transitions, such as up-conversion. This problem can be circumvented by coordinating organic molecules containing chromophore groups to Er(III), thereby improving the potential applications.[2] Metalloporphyrins, including transition metals, are well characterized as efficient light harvesting molecules that mimic natural systems.[3] We previously investigated the optical optimization of Er(III)-based complexes by coordinating Pt(II)− and Zn(II)−porphyrin ligands with aryl−ether dentrons.[3a,4] The heavy Pt(II) atom provides the Pt(II)−porphyrin complex with a higher intersystem crossing (ISC) efficiency for the singlet-to-triplet state transition compared with that of the Zn(II)−porphyrin complex. The experimentally observed energy transfer between the Pt(II)−porphyrin derivative and Er(III) is believed to play a key role in the luminescence efficiency of the Er(III) complex. However, the spectroscopic properties of metalloporphyrins coordinated to lanthanides are poorly characterized.

A more complete understanding and analysis of the energy transfer process taking place between the organic ligands and the lanthanide ions are warranted to improve their application in optical telecommunications. Although many theoretical models attempt to rationalize the mechanism of energy transfer between the organic ligands and Ln(III), they focus almost exclusively on visible luminescence.[5] We extensively characterized the photophysical properties of Er(III) complexes coordinated to the mixed ligands Pt(II)−porphyrin derivative, Pt[5,10,15-triphenyl-20(4-caboxylphenyl)-porphyrin] (PtP), and terpyridine (tpy). Both PtP and tpy contributed an antenna effect to Er(III), but the energy transfer from PtP predominated. In this study, we experimentally and theoretically investigated the pathway of energy transfer from PtP to Er(III).

Experimental Methods

Synthesis. The synthesis of Pt−porphyrin and Er(III) complexes[3a] and the preparation of Pt−porphyrin from free-base porphyrin were previously reported.[3a,4] A mixture of carboxylated Pt−porphyrin (3 equiv) and KH (3.3 equiv) was added to freshly distilled tetrahydrofuran (THF; J. T. Baker) and stirred overnight at room temperature until H_2 generation ceased. After both salts were depleted, a solution of anhydrous $ErCl_3$ (1 equiv) and terpyridine (1 equiv) in methanol was added and stirred for an additional 48 h. The resulting solution was filtered, and the solvent was removed. The resultant solid was washed sequentially with methanol and diethyl ether. We synthesized 9-coordinated [Er(PtP)$_3$(tpy)] as $C_{150}H_{92}ErN_{15}O_6Pt_3$ according to Scheme 1.

Pt—Porphyrin-Ligand. ^{1}H NMR ($CDCl_3$, ppm): δ 8.76 (s, 6H, β-pyrrole), 8.69 (d, 2H, β-pyrrole), 8.50 (d, 2H, Ar−H), 8.30 (d, 2H, Ar−H), 8.27 (d, 6H, Ar−H), 7.75 (m, 9H, Ar−

* To whom correspondence should be addressed. E-mail: jgkang@cnu.ac.kr (J.-G.K.), hkk777@korea.ac.kr (H.K.K.). Phone: +82-42-821-6548 (J.-G.K.), +82-41-860-1493 (H.K.K.). Fax: +82-42-821-8896 (J.-G.K.), +82-41-867-5396 (H.K.K.).

† Hannam University.

‡ Chungnam National University.

Current address. Department of Chemistry, Korea University, Jochiwon, Chungham 339-700, Korea.

§ Yonsei University.

10.1021/jp0688512 CCC: $37.00
Published on Web 06/26/2007

SCHEME 1

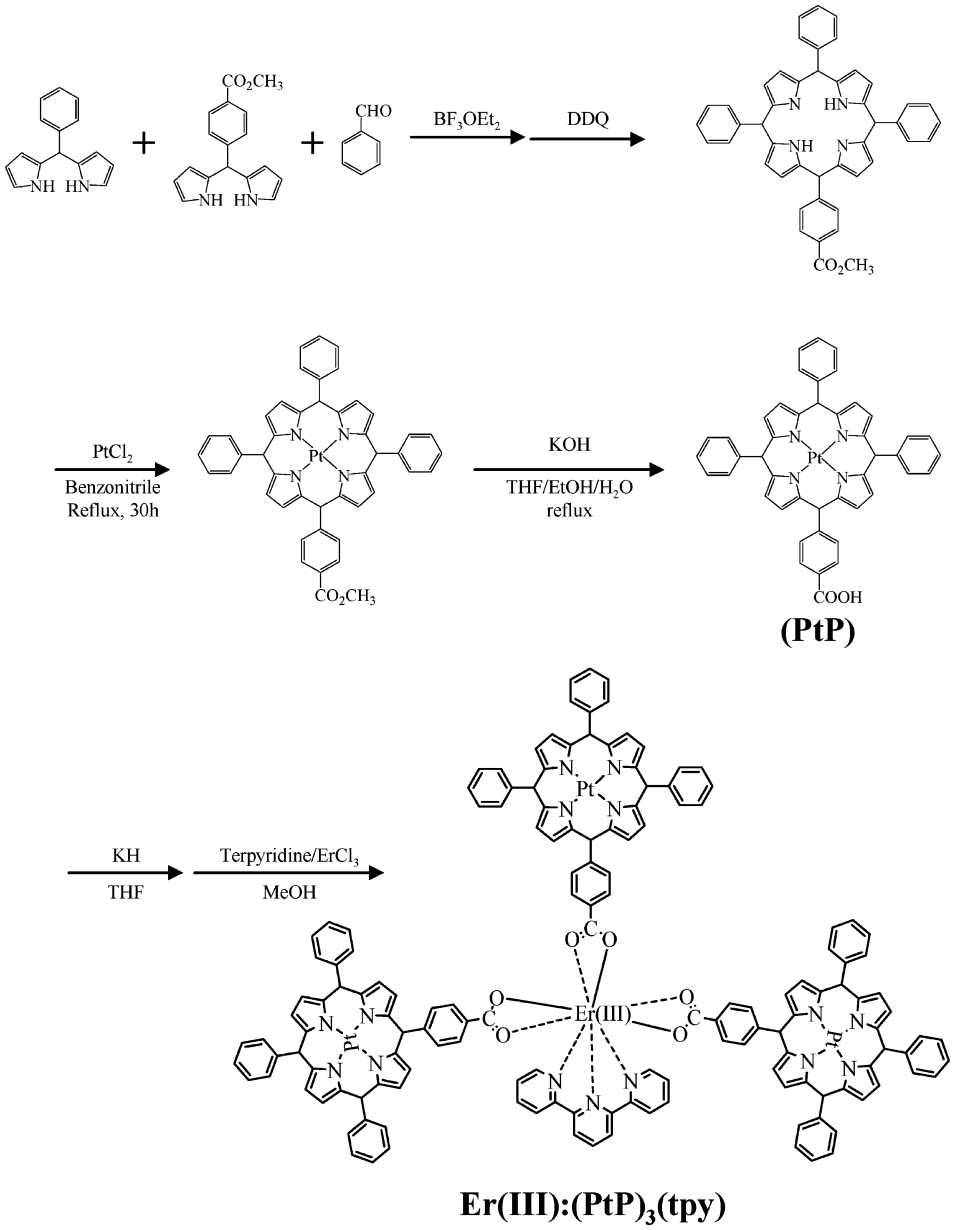

H). FT-IR (KBr, cm^{-1}): 3400, 1690, 1360, 1020. EI-MS (*m*/*z*): calcd for $C_{45}H_{28}N_4O_2Pt$, 851.19; found, 851.

[Er(PtP)$_3$(tpy)]. FT-IR (KBr, cm^{-1}): 1595, 1414. Anal. Calcd (%) for $C_{150}H_{92}ErN_{15}O_6Pt_3$: C, 61.01; H, 3.14; N, 7.11; Er, 5.66. Found: C, 60.62; H, 3.74; N, 6.80; Er, 6.17.

Photophysical Measurements. The UV−vis spectra of free PtP and the Er(III) complex were recorded at room temperature on a Shimadzu UV-2401PC spectrophotometer with a 1 cm path-length quartz cell. The excitation and luminescence spectra of free PtP and the Er(III) complex were measured on a steady-state fluorospectrometer (Edinburgh Instruments, FS920) equipped with a 450 W Xe lamp. The luminescence spectra in the visible region were recorded with a PMT system (Hamamatsu, R955), and the luminescence spectra in the near-infrared (NIR) region were recorded with a Ge-detector (Edinburgh Instruments, EI-L) cooled by liquid nitrogen.

The quantum yield of the visible luminescence for each sample (Φ_s) was determined by the relative comparison procedure, using a reference of a known quantum yield (quinine sulfate in diluted H_2SO_4 solution, $\Phi_r = 0.546$). The general equation used in the determination of relative quantum yield[6] is given as follows:

$$\Phi_s = \Phi_r\left(\frac{A_r(\lambda_r)}{A_s(\lambda_s)}\right)\left(\frac{I(\lambda_r)}{I(\lambda_s)}\right)\left(\frac{n_s^2}{n_r^2}\right)\left(\frac{D_s}{D_r}\right) \quad (1)$$

In eq 1, $A(\lambda)$ is the absorbance, $I(\lambda)$ is the relative intensity of the exciting light at wavelength λ, n is the average refractive index of the solvent, and D is the integrated area under the corrected emission spectrum.

For time-decay measurements, a high power nanosecond Nd:YAG laser system (355 nm, EXPLA, NT342) was used with a pump wavelength selected within the third-harmonic generation. The laser output has a pulse width of ~5 ns with a repetition rate of 10 Hz. The final pump laser pulse was adjusted to a wavelength of 416 nm using the hydrogen gas-filled Raman shifter. The final pump power on the sample surface was adjusted to but not exceeding about 0.5 mJ per pulse. The visible luminescence decay signals from the sample were detected on the right angle by a PMT system

(Hamamatsu, R928) after dispersion by a 300 mm monochromator (Acton Research Cooperation, SpectraPro 2300i). Detection in the near-infrared region was achieved by a thermoelectric (TE) cooled near-infrared PMT system (Hamamatsu, H9170-75). The electric output signals were collected with a digital oscilloscope system (Agilent Infiniium, 54832B). All samples were diluted in THF for spectroscopic measurement, and the concentrations were adjusted to approximately 10^{-5} M. The sample solutions were deoxygenated by degassing four times with freeze−pump−thaw cycles on a high-vacuum line with liquid nitrogen.

Time-resolved triplet−triplet absorption spectra were measured by using a xenon lamp as a probe source. The probe light from the xenon lamp was shaped by an iris and then perpendicularly focused into the sample which was excited by the pump beam from the Nd:YAG laser system (BMI series, 7 ns fwhm pulse) pumped with optical parametric oscillator (OPO) laser (B.M. Industries OP901-355, 5 ns fwhm pulse). The transmitted beam was collected by focusing optics and then detected with a monochromator (Jobin Yvon, H20) and PMT (Hamamatsu, R928). The signals were processed by a 500 MHz digital oscilloscope (Hewlett-Packard, 54520A) and transferred to a computer.[7a] Time-resolved triplet−triplet absorption signals were fitted by a monoexponential decay. From the fitted data, the zero time intensity of the time-resolved triple−triplet signal was estimated to obtain the zero-time transient triplet absorbance (ΔOD). Triplet quantum yields (Φ_T) were determined by the power dependent comparative method which has the following relationship between excitation energy (E) and difference in zero-time transient triplet absorbance (ΔOD):[7]

$$\Delta\mathrm{OD} = a(1 - \exp(-bE)) \tag{2}$$

In eq 2, a is a proportionality constant and b is equal to $k\Phi_T$ (Φ_T is a triplet quantum yield, ϵ_g is an absorption coefficient of the transition, and k is an instrumental constant). With the reported value ($\Phi_T^R = 0.72$) of the reference H_2TPP (5,10,15,-20-tetraphenylporphyrin) and the estimated values of b and ϵ_g for both reference and sample, the triplet quantum yield of sample was calculated as the following:[7]

$$\Phi_T^S = \Phi_T^R \frac{b^S \epsilon_g^R}{b^R \epsilon_g^S} \tag{3}$$

In eq 3, S and R stand for sample and reference, respectively.

Theoretical Models. Most energy transfer processes can be understood in terms of their mechanisms for electrostatic interaction and resonance transfer. For the electrostatic interaction, a power series expansion of the reciprocal of the distance between the sensitizer and acceptor was used to explain the dipole−dipole and dipole−multipole interactions.[8] The energy transfer rates for Ln(III) complexes were evaluated as

$$W_{ET}^{mp} = \frac{2\pi}{\hbar} \frac{e^2 S_L}{(2J+1)G} F \sum_\lambda \gamma_\lambda \langle \alpha' J' || U^{(\lambda)} || \alpha J \rangle^2 \tag{4}$$

for the dipole−multipole (mp) mechanism, with $\lambda = 2$, 4, and 6, and

$$W_{ET}^{dd} = \frac{2\pi}{\hbar} \frac{e^2 S_L}{(2J+1)G R_L^{\,6}} F \sum_\lambda \Omega_\lambda^{ed} \langle \alpha' J' || U^{(\lambda)} || \alpha J \rangle^2 \tag{5}$$

for the dipole−dipole (dd) mechanisms by taking into account the energy mismatch factor (F).[5] Energy mismatch factors were determined from the experimental data according to

$$F = \frac{1}{\hbar \Delta A_L} \sqrt{\frac{\ln 2}{\pi}} \exp\left[-\left(\frac{\Delta E}{\hbar \Delta A_L} \right)^2 \ln 2 \right] \tag{6}$$

In eq 6, ΔE is the energy difference between the ligand donor level and the lanthanide ion acceptor level, and ΔA_L is the bandwidth at half-height of the ligand state. The term was multiplied according to the appropriate Boltzmann distribution to account for the back-transfer process. The quantities $\langle ||\, || \rangle$ are reduced matrix elements of the unit tensor operators, $U^{(\lambda)}$,[9] and the dipole strength, S_L, can be evaluated using the radiative lifetime, τ_L^R, of the state $|L\rangle$ of the donor ligand and the fluorescence energy σ (in cm^{-1}) as

$$\frac{1}{\tau_L^R} = \frac{32}{3} \frac{\pi^3 \sigma^3}{\hbar} S_L \tag{7}$$

The major difference between the mp and dd mechanisms is the distance dependence, R_L, between the lanthanide ion nucleus and the ligand donor atom. For the mp mechanism, γ_λ in eq 4 is described as

$$\gamma_\lambda = (\lambda + 1) \frac{\langle r^\lambda \rangle^2}{(R_L^{(\lambda+2)})^2} \langle 3 || C^{(\lambda)} || 3 \rangle^2 (1 - \sigma_\lambda)^2 \tag{8}$$

which includes the reciprocal of $(R_L^{(\lambda+2)})^2$ with the radial expectation value of r^λ, $\langle r^\lambda \rangle$, for 4f electrons and the Racah tensor operator $C^{(\lambda)}$. For the dd mechanism, the rate given by eq 5 is proportional to the reciprocal of $R_L{}^6$, the Judd−Ofelt intensity parameters, Ω_λ^{ed}, which can be evaluated from the oscillator strength of the absorption spectrum. In eqs 4 and 5, the reduced matrix elements of the unit tensor apply $J + J' \geq \lambda \geq |J + J'|$ as the significant selection rule for the mp and dd mechanisms.

Conversely, a resonance energy transfer occurs when the energy difference between the ground and excited states of the sensitizer and acceptor systems is aligned properly. The rate of resonance energy transfer was rendered in terms of induced dipole (Förster type) and electron exchange (Dexter type) mechanisms. The transfer rate for the exchange mechanism was previously defined by the selection rule $\Delta J = 0, \pm 1$, in accordance with the lanthanide ion's total spin operator.[5c] However, applying the selection rule can be controversial because the exchange interaction is active when the emission band of a sensitizer (S) overlaps the 4f−4f absorption band of the lanthanide ion. The rate dependence on the distance between the sensitizer and acceptor is greater for the Dexter-type mechanism than the Förster type. However, the Förster type proves more reliable in the solution state. The energy transfer rate, W_{ET}^{res}, for the Förster type can be expressed by[10]

$$W_{ET}^{res} = \frac{1}{\tau_D} \left(\frac{R_0}{R_L} \right)^6 \tag{9}$$

where τ_D is the decay time of the donor in the absence of an acceptor. In eq 9, R_0 is the critical distance (Å), which is expressed by

$$R_0 = 0.211[\kappa^2 n^{-4} \Phi_D \textstyle\int F_D(\lambda) \epsilon_A(\lambda) \lambda^4 \, d\lambda]^{1/6} \tag{10}$$

In the equation above, κ^2 describes the relative orientation in space of the transition dipoles of the donor and acceptor and

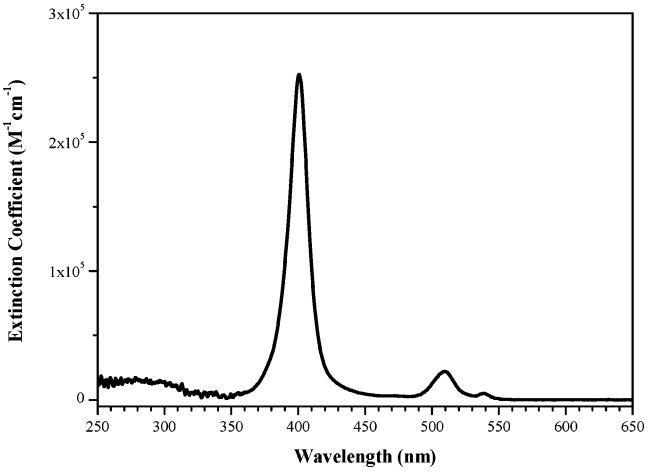

Figure 1. Absorption spectra of PtP in THF.

TABLE 1: Absorption Peak Wavelengths and Extinction Coefficients of PtP and [Er(PtP)$_3$(tpy)] Dissolved in Deoxygenated THF (λ_{max}, nm; ϵ, M^{-1} cm^{-1})

	B-band		Q-band (1,0)		Q-band (0,0)	
materials	λ_{max}	ϵ	λ_{max}	ϵ	λ_{max}	ϵ
PtP	400	252 600	510	22 000	539	5 200
Er(III)(PtP)$_3$(tpy)	400	720 800	510	63 100	539	15 000

is usually assumed to be equal to $^2/_3$; n is the refractive index of the medium, and Φ_D is the quantum yield of the donor in the absence of an acceptor. The integral is over the normalized emission band shape of the sensitizer, $F_D(\lambda)$, and the normalized absorption band of the acceptor, $\epsilon_A(\lambda)$.

Results and Discussion

Absorption Spectrum. The absorption spectrum of the free PtP dissolved in THF is shown in Figure 1. The spectral shapes of PtP and [Er(PtP)$_3$(tpy)] were almost identical, apart from their relative intensities. The absorption spectrum of [Er(PtP)$_3$(tpy)] lacked the characteristic f → f sharp lines in the range of 250−600 nm due to the relatively small extinction coefficient of Er(III). Both PtP and [Er(PtP)$_3$(tpy)] produced a very strong B-band at 400 nm and two weak Q-bands at 510 and 540 nm. The B-band represents the transition from the ground state to the second excited singlet state (S_2), and the Q-bands reflect the transition from the ground state to the first excited singlet (S_1). The doublet structure of the Q-band has a strong dependence on the vibronic distortions of the first excited state. The extinction coefficients for the absorption bands are listed in Table 1. The three PtP ligands within [Er(PtP)$_3$(tpy)] do not alter the absorption features of Er(III), suggesting that the energy states of PtP in [Er(PtP)$_3$(tpy)] are not influenced by Er(III).

Luminescence and Excitation Spectra. The luminescence spectrum of free PtP was measured under both air-saturated and deoxygenated conditions. As shown in Figure 2, the B-band excitation of the deoxygenated PtP solution produced a strong band at 665 nm and a weak band at 730 nm. The Q-band excitation had an identical spectral shape. The two luminescence bands were quenched considerably by oxygen under air-saturated conditions. The excitation spectrum of the PtP solution was also measured at 660 nm under deoxygenated conditions, and the two observed excitation spectra aligned properly with the B- and Q-bands of the absorption spectrum (Figure 2). Interestingly, the luminescence spectrum resembled the mirror image of the Q-absorption band. The quenching effect of oxygen and the large Stoke's shift within the mirror image strongly

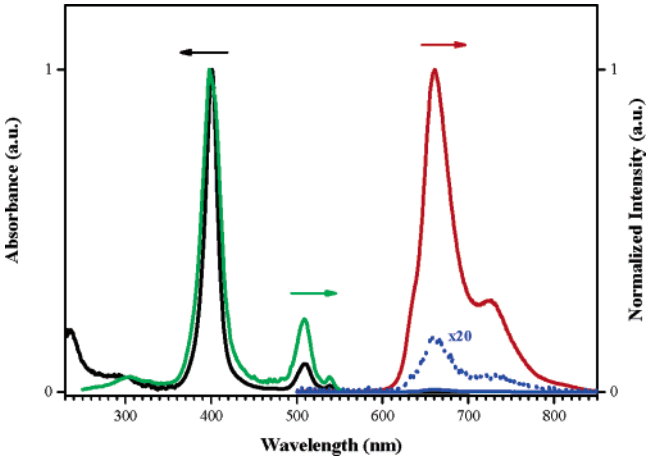

Figure 2. Absorption (black line), luminescence (λ_{exc} = 405 nm, red line), and excitation (λ_{ems} = 660 nm, green line) spectra of PtP under deoxygenated conditions. The blue dotted line represents the luminescence spectrum obtained under air-saturated conditions (λ_{exc} = 405 nm).

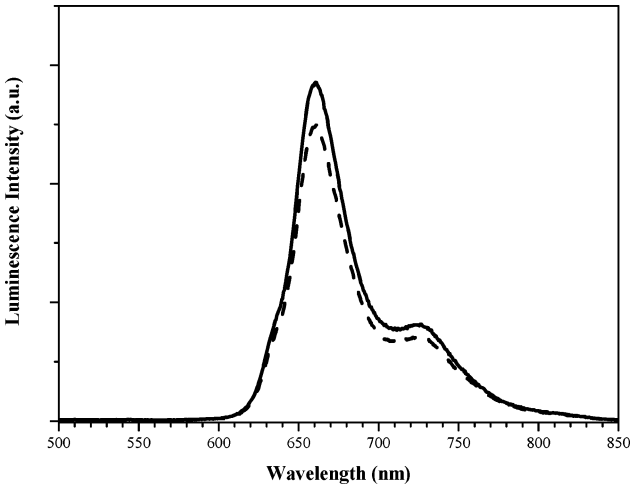

Figure 3. Luminescence spectra of PtP (solid line) and [Er(PtP)$_3$(tpy)] complexes (dashed line) in the visible region.

suggest that the observed luminescence to phosphorescence originated from the first triplet excited state (T_1).

The luminescence spectrum of [Er(PtP)$_3$(tpy)] dissolved in THF was measured under deoxygenated conditions. As shown in Figures 3 and 4, the B-band excitation produced strong PtP phosphorescence in the 600−850 nm region and weak NIR luminescence in the 1350−1700 nm region. This NIR luminescence was characteristic of the transition from the emitting $^4I_{13/2}$ level to the $^4I_{15/2}$ ground level of Er(III). The excitation spectrum of the NIR emission was also measured under deoxygenated conditions. As shown in Figure 4, the excitation spectrum of the NIR luminescence resembled the absorption spectrum of PtP, suggesting that an energy transfer occurred from PtP and Er(III). For [Er(PtP)$_3$(tpy)], the oscillator strength of the phosphorescence decreased by ~13% relative to that of free PtP. The decrease in PtP phosphorescence was proportional to the energy transfer from PtP to Er(III). We also recorded the luminescence spectrum of [Er(PtP)$_3$(tpy)] under air-saturated conditions (Figure 4), which revealed no NIR emission. Hence, the surrounding oxygen molecules must have seriously influenced the energy transfer process.

Decay Times and Quantum Yields of Triplet State and Sensitized Luminescence. The phosphorescence decay time of PtP was measured under both air-saturated and deoxygenated

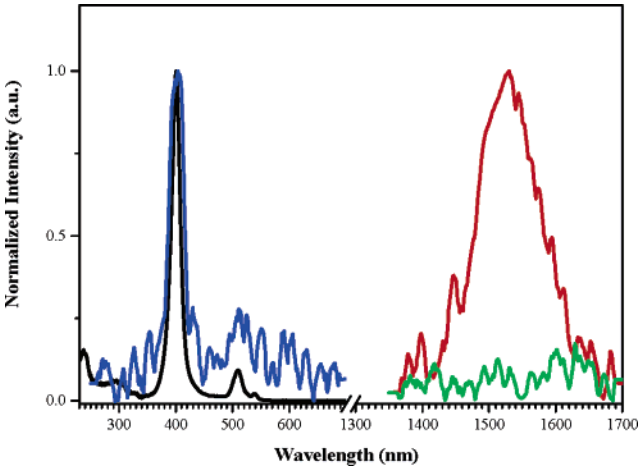

Figure 4. NIR luminescence (λ_{exc} = 405 nm, red line), excitation (λ_{ems} = 1530 nm, blue line), and absorption (black line) spectra of [Er(PtP)$_3$(tpy)] under deoxygenated conditions. The green line represents the luminescence spectrum obtained under air-saturated conditions.

conditions. The decay time of phosphorescence at 660 nm fit the profile for a single-exponential component. The decay time was evaluated for ~300 ns under air-saturated conditions and 39 μs under deoxygenated conditions. From these results, the oxygen diffusion-controlled quenching rate constant, k_{diff}, was determined using the following equation:

$$\frac{\tau_0}{\tau} = 1 + k_{diff}\tau_0[Q] \qquad (11)$$

where τ_0 and τ are the decay times in the absence and presence of the quencher, respectively, and [Q] represents the concentration of the quencher. When the maximum concentration of oxygen in THF was adjusted to 9.9 × 10^{-3} M L^{-1} at the standard state,[11] we obtained k_{diff} = 3.3 × 10^8 L s^{-1} M^{-1}.

The Er(III) complex profile for the time decay of phosphorescence under air-saturated conditions was also quenched by oxygen, which also quenched the energy transfer process. However, the time decay phosphorescence profile of the Er(III) complex was remarkably different from that of free PtP under deoxygenated conditions, as shown in Figure 5a. As listed in Table 2, the decay profile was fit to a double-exponential component as τ_1 = 3.6 μs with 11% amplitude and τ_2 = 39 μs. We also prepared [Gd(PtP)$_3$(tpy)] to confirm the two decay times of phosphorescence for the Er(III) complex. The Gd(III) complex is commonly used as a model system owing to its lack of energy transfer as a result of its emitting level having higher energy (about 32 200 cm^{-1}) than the singlet states for the organic sensitizers. As shown in Figure 5a, the time profile for [Gd(PtP)$_3$(tpy)] phosphorescence was identical to that of free PtP, with no initial burst component. The phosphorescence decay profiles of the samples were also measured at liquid nitrogen temperature (LNT), giving profiles identical to those measured at room temperature for all samples (Figure 5b). We also measured the decay profiles of the two complexes and the free PtP ligand dissolved in deoxygenated toluene at room and liquid nitrogen temperatures. For [Er(PtP)$_3$(tpy)], the fast decay-component was also observed at the two temperatures and the results are listed in Table 2. Ruling out any experimental uncertainty in the decay profile of [Er(PtP)$_3$(tpy)], we assumed that the fast decay time could be related to the energy transfer process.

We also measured the decay curve of the sensitized NIR emission from [Er(PtP)$_3$(tpy)] by exciting within the B-band.

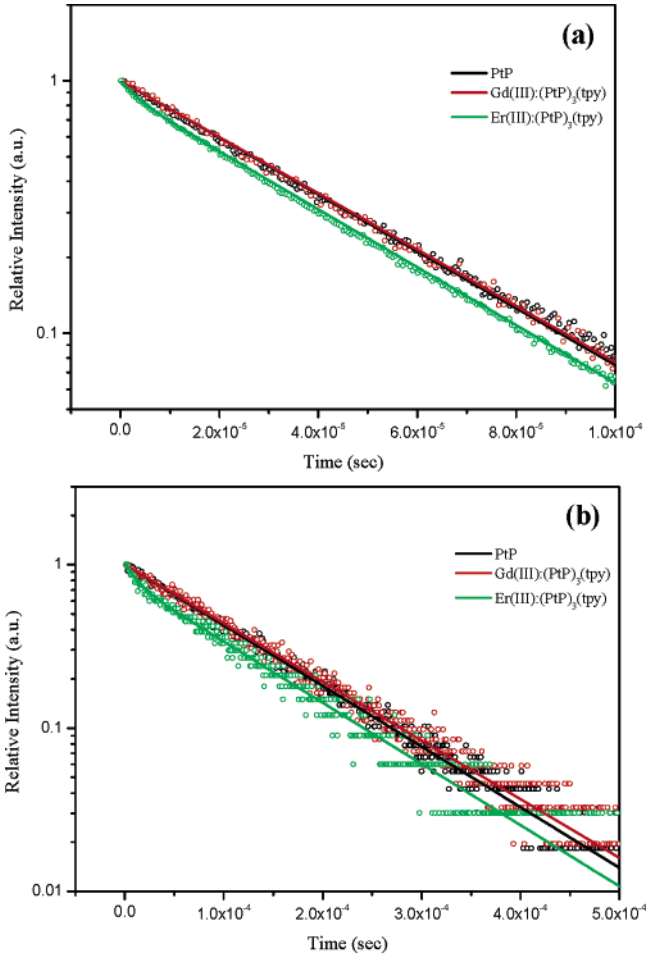

Figure 5. The luminescence decay profiles of phosphorescence measured from PtP, [Gd(PtP)$_3$(tpy)], and [Er(PtP)$_3$(tpy)] at (a) room temperature and (b)liquid nitrogen temperature.

TABLE 2: Phosphorescence Lifetimes of [Ln(PtP)$_3$(tpy)] Dissolved in Deoxygenated THF and Toluene Measured at Room Temperature (RT) and Liquid Nitrogen Temperature (Degassed Condition)[a]

		τ_{obs} (μs)	
solvent	[Ln(PtP)$_3$(tpy)]	RT	LNT
THF	Gd	39	121
	Er	3.6 (0.11) + 39 (0.89)	11 (0.22) + 116 (0.78)
toluene	Gd	38	122
	Er	6.0 (0.16) + 41 (0.84)	9.0 (0.18) + 118 (0.82)

[a] The values given in parentheses are the amplitude ratios. λ_{exc} = 405 nm and λ_{ems} = 660 nm.

The decay curve was reproducible using a single-exponential component, and the decay time of the sensitized NIR emission was determined as τ_{sen} = 1.2 μs. The quantum yield of the sensitized NIR luminescence of Ln(III) in the complex can be estimated using the relationship between the experimentally determined lifetime of Ln(III) (τ_{obs}) and its natural lifetime (τ^{Ln}),[12] represented as

$$\Phi_{sens} = \frac{\tau_{obs}}{\tau^{Ln}} \qquad (12)$$

Using the reported τ^{Ln} value of 8.00 ms for Er(III),[13] we determined the quantum yield (Φ_{Ln}) of the sensitized luminescence to be ~0.015%. The quantum yield of the sensitized luminescence of [Er(PtP)$_3$(tpy)] was very close to the literature values of 0.01−0.04% for Er(III) organic complexes.[14]

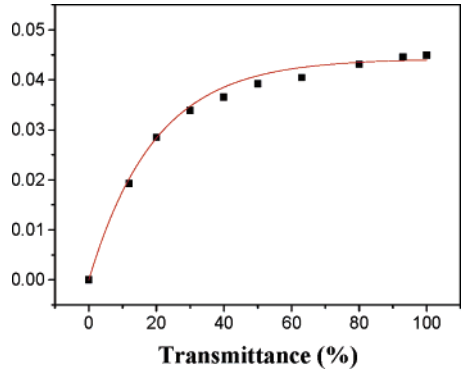

Figure 6. Excitation power-dependence of the zero-point ΔOD for [Er(PtP)$_3$(tpy)] dissolved in deoxygenated toluene.

TABLE 3: Quantum Yields of [Ln(PtP)$_3$(tpy)] Complexes Dissolved in Deoxygenated THF

	quantum yield			
[Ln(PtP)$_3$(tpy)]	Φ_{phos}	Φ_{ET}	Φ_{sens}	Φ_T
Gd	0.424			0.35
Er	0.372	0.123	1.50×10^{-4}	0.36

We also measured the quantum yields of the phosphorescence of [Gd(PtP)$_3$(tpy)] and [Er(PtP)$_3$(tpy)]. As listed in Table 3, the quantum yield of [Er(PtP)$_3$(tpy)] was decreased by approximately 12% relative to that of the Gd(III) complex, due to the energy transfer from PtP to Er(III). The sensitized luminescence through the triplet T_1 state of PtP consists of the conversion of the B-band excitation of PtP into the triplet T_1 state via the relaxation and intersystem crossing processes, the energy transfer from the singlet to the resonance level of Ln(III), and the subsequent relaxation to the emitting level. Considering this pathway, the overall quantum yield of the sensitized luminescence can be expressed as

$$\frac{\tau}{\tau_0} = \Phi_{antenna}\Phi_{ET}\Phi_{rel} \qquad (13)$$

where the quantum yield of the Gd(III) complex is taken as $\Phi_{antenna}$ and Φ_{rel} is the relaxation efficiency strongly associated with a radiationless transition. Substituting the experimentally determined values of $\Phi_{antenna}$ and Φ_{ET} into eq 13, we obtained $\Phi_{rel} = 0.29\%$. This low efficiency for the relaxation from receiving levels to the emitting $^4I_{13/2}$ level of Er(III) may be due to the larger energy gap (ΔE) between the T_1 excited state of PtP and the emitting level of the Er(III) ion: $\Delta E \cong 9040$ cm^{-1}.

In addition, we also determined the triplet quantum yields (Φ_T) of [Gd(PtP)$_3$(tpy)] and [Er(PtP)$_3$(tpy)] to confirm whether the singlet state of PtP might be involved in the energy transfer. Time-resolved triplet−triplet absorption signals were measured at 450 nm with the excitation of 510 nm as a function of the energy of the laser pulse. Figure 6 shows a typical excitation power-dependence of the zero-time triplet ΔOD. With the measured values of the zero-time triplet ΔOD for both the reference and the sample, the triplet quantum yield was calculated using eq 3. As listed in Table 3, the triplet quantum yield of the PtP ligand in [Er(PtP)$_3$(tpy)] is almost equal to that in [Gd(PtP)$_3$(tpy)]. These results led us to rule out the possibility for the energy transfer from the singlet excited state of the PtP ligand to the Er ion.

Modeling the Energy Transfer Process. We estimated the energy transfer rate using eqs 4, 5, and 9 to elucidate the energy transfer pathway. The parameters for the calculations are listed in Table 4. To determine which excited levels of Er(III) were involved in the energy transfer from PtP, we applied the energy mismatch factor (F), the selection rules ($|\Delta J| = 2, 4, 6$) for the mp and the dd mechanisms, and the sufficient spectral overlap between the phosphorescence band of PtP and the f → f absorption band of the Er(III) ion for the resonance energy transfer.

As described in eq 6, the factor F is determined by the energy difference (ΔE) between the energy donor level and energy acceptor level and by the half-width (ΔA_L). We obtained $\Delta A_L(^3\pi\pi^*) = 1025$ cm^{-1} from the phosphorescence spectrum and $\Delta A_L(^1\pi\pi^*) = 1560$ cm^{-1} from the absorption band. We

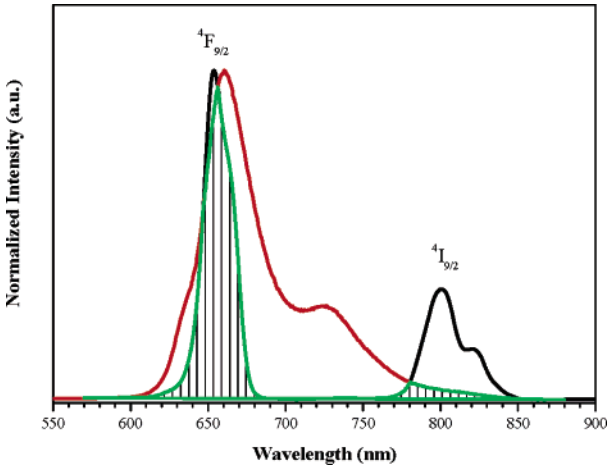

Figure 7. Spectral overlap (shaded area) between the luminescence spectrum of PtP and the absorption spectrum of Er(NO$_3$)$_3$ in aqueous solution (black line).

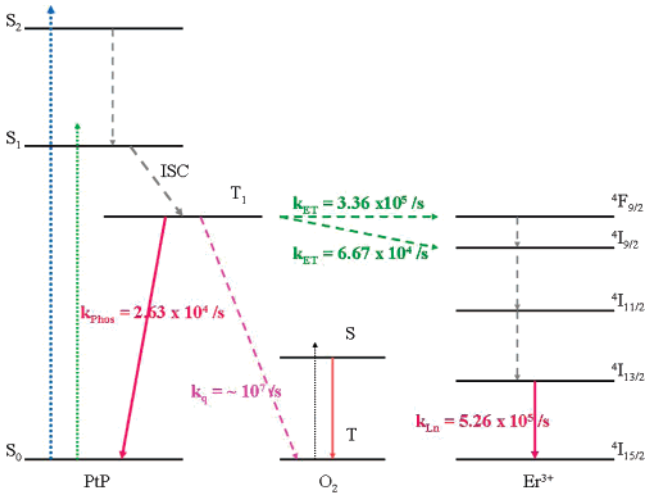

Figure 8. Schematic of the energy transfer process of [Er(PtP)$_3$(tpy)] in tetrahydrofuran solution.

TABLE 4: Parameters Used in the Calculation of the Energy Transfer Rate Constants

	λ		
	2	4	6
$\langle r^\lambda \rangle^a$	1.937×10^{-17} cm^2	9.945×10^{-34} cm^4	1.056×10^{-49} cm^6
$\langle 3\|\|C^{(\lambda)}\|\|3\rangle^{2\ b}$	1.866	1.272	1.613
$\sigma_\lambda{}^c$	0.686	0.139	−0.190
$R_L \approx 11.4$ Å^d			
$S_L(^1\pi\pi^*) \approx 5.18 \times 10^{-15}$ esu^2 cm^2			
$S_L(^3\pi\pi^*) \approx 1.29 \times 10^{-22}$ esu^2 cm^2			

[a] From ref 15. [b] From ref 5d. [c] From ref 16. [d] The distance between the lanthanide ion and PtP (R_L) was determined from theoretical geometry optimization with the molecular mechanics MM+ method.

TABLE 5: Calculated Energy Transfer Rate Constants for the Electrostatic Interaction Mechanism in [Er(PtP)$_3$(tpy)]

donating state (E/cm^{-1})		accepting state (E/cm^{-1})	dipole−dipole[a] k_{ET} forward/s^{-1}	dipole−dipole[a] k_{ET} backward[b]/s^{-1}	dipole−2$^{\lambda}$pole k_{ET} forward/s^{-1}	dipole−2$^{\lambda}$pole k_{ET} backward[b]/s^{-1}
$^1\pi\pi^*$(19 390)	→	$^4F_{7/2}$ (20 500)	2.40×10^{-28}	2.52×10^{-26}	9.11×10^{-22}	9.57×10^{-20}
$^1\pi\pi^*$(19 390)	→	$^2H_{11/2}$ (19 200)	7.66×10^{-15}	2.97×10^{-15}	6.72×10^{-4}	2.60×10^{-4}
$^1\pi\pi^*$(19 390)	→	$^4S_{3/2}$ (18 400)	7.84×10^{-26}	3.40×10^{-28}	3.56×10^{-22}	1.54×10^{-24}
$^3\pi\pi^*$(15 580)	→	$^4I_{11/2}$ (10 250)	1.15×10^{-114}	7.81×10^{-124}	1.15×10^{-104}	7.81×10^{-114}

[a] $\Omega_{2,4,6} = 2 \times 10^{-20}$ cm^{-1} from ref 17. [b] The backward transfer rates were calculated by multiplying the forward rates by the Boltzmann factors at room temperature.

TABLE 6: Calculated Energy Transfer Rate Constants for the Förster Resonance Energy Transfer Mechanism in [Er(PtP)$_3$(tpy)]

	accepting state		
	$^4F_{9/2}$	$^4I_{9/2}$	total
spectral overlap integral (M^{-1} cm^{-1} nm^4)	4.16×10^{12}	8.23×10^{11}	4.98×10^{12}
R_0 (Å)	17.43	13.31	17.97
k_{ET} (s^{-1})	3.36×10^5	6.67×10^4	4.04×10^5
ratio (%)	83.44	16.56	100.00

determined the energy mismatch factor to be almost zero using these values, when ΔE exceeds 4000 cm^{-1}. Ultimately, only four levels, $^4F_{7/2}$, $^2H_{11/2}$, $^3S_{3/2}$, and $^4I_{11/2}$, could be considered as energy acceptor levels in order for the mp and the dd mechanisms to prove true. When the additional activation arising from the spectral overlap was neglected, the selection rule for the exchange mechanism was previously given by $|\Delta J| = 0$ and 1 for the pure exchange mechanism. Only the $^4I_{13/2}$ level of Er(III) is suitable for the exchange mechanism; however, the energy difference between this level and the singlet or triplet excited states of PtP is too great for $^4I_{13/2}$ to be considered an acceptor level. Hence, the pure exchange mechanism was ruled out for [Er(PtP)$_3$(tpy)]. To simplify the calculations, several conditions were assumed based on experimental results; the energy donor level is the first singlet excited state (19 400 cm^{-1}) or the triplet excited state (14 600 cm^{-1}) of PtP. The $^4F_{7/2}$ (20 500 cm^{-1}), $^2H_{11/2}$ (19 200 cm^{-1}), and $^4S_{3/2}$ (18 400 cm^{-1}) levels of Er(III) ions are possible to be acceptor levels from the first excited singlet level of PtP, and $^4I_{11/2}$ (10 250 cm^{-1}) would be a suitable acceptor level from the triplet excited level of PtP. The theoretical values for the forward and back-transfer rate constants calculated from eqs 4 and 5 are listed in Table 5. The calculated rate constants were unreasonably small. Although the transition from the singlet state of PtP to the $^2H_{11/2}$ level of Er(III) ions was large, it was not involved in the energy transfer pathway. Consequently, electrostatic interactions are not responsible for the energy transfer processes occurring in the [Er(PtP)$_3$(tpy)] complex.

We were then interested in the $^4F_{9/2}$ (15 300 cm^{-1}) and $^4I_{9/2}$ (12 500 cm^{-1}) levels of the Er(III) ion, which were excluded in the mp and dd calculations although their absorption bands overlapped with the phosphorescence band, as shown in Figure 7. Using eqs 9 and 10, we calculated the resonance energy transfer rate constant relative to the spectral overlap between the absorption of Er(III) ion and the luminescence of PtP. We normalized the $^4I_{15/2} \rightarrow {}^4F_{9/2}$ (15 300 cm^{-1}) and $^4I_{9/2}$ (12 500 cm^{-1}) absorption bands overlapping the phosphorescence band and evaluated the overlap integrals. Finally, using $\kappa^2 = {}^2/_3$, $n = 1.407$ in THF, and $\Phi_D = 0.45$,[18] we evaluated the critical distances and the rate constants (Table 6). The average critical distance was 17.8 Å, which is considerably larger than the R_L of 11.4 Å, indicating that the resonance energy transfer mechanism is reasonable for this complex system. As listed in Table 6, the total resonance energy transfer rate constant from the triplet state to Er(III) is 4.04×10^5 s^{-1}. The $^4F_{9/2}$ state of [Er(PtP)$_3$(tpy)] acted as the main receiving level, with 83% of the energy being transferred from the triplet state to the $^4F_{9/2}$ level and the remaining 17% of the energy being transferred to the $^4I_{9/2}$ state. The rate was calculated to be in the order of 10^5 s^{-1}, considerably smaller than the rate of 10^7 s^{-1} when quenched by oxygen. The small rate constant reflects the suppression of the quenching by oxygen within the energy transfer process of Er(III). Figure 8 shows the three steps in the main pathway of the sensitized luminescence of the [Er(PtP)$_3$(tpy)] complex. The B-band ($S_0 \rightarrow S_2$) excitation of PtP is nonradiatively relaxed to the S_1 state, which is followed by the subsequent intersystem crossing of the S_1 state to its T_1 state and energy transfer from the triplet state to the near-resonant $^4F_{9/2}$ state of Er(III).

Conclusion

This study revealed that Er(III) complexed with PtP and tpy can produce sensitized NIR luminescence by energy transfer from PtP to the Er(III) ion. Our theoretical calculations confirmed that Förster resonance energy transfer correctly explains the energy transfer rate constants for the Er(III) complex dissolved in THF. We demonstrated that the main energy transfer occurred by resonance from the triplet state of PtP to the $^4F_{9/2}$ state and also to the $^4I_{9/2}$ state.

Acknowledgment. This work was financially supported by the Korean Ministry of Science and Technology through the National Research Laboratory Program at Hannam University. J.-G.K. and M.-K.N. acknowledge the research grants from Chungnam National University and Alti-Electronics Co., Ltd. Y.-R.K. acknowledges a grant from the Korea Science and Engineering Foundation (KOSEF) (Grant No. R0A-2003-000-10305-0). K.-H.C. acknowledges the fellowships of the BK 21 program from the Ministry of Education and Human Resources Development.

References and Notes

(1) (a) Bünzli, J.-C. G.; Piguet, C. *Chem. Soc. Rev.* **2005**, *34*, 1048. (b) Xiao, M.; Selvin, P. R. *J. Am. Chem. Soc.* **2001**, *123*, 7067. (c) Pfeiffer, D.; Ximba, B. J.; Liable-Sands, L. M.; Rheingold, A. L.; Heeg, M. J.; Coleman, D. M.; Schlegel, H. B.; Kuech, T. F.; Winter, C. H. *Inorg. Chem.* **1999**, *38*, 4539. (d) Werts, M. H. V.; Hostraat, J. W.; Geurts, F. A. J.; Verhoeven, J. W. *Chem. Phys. Lett.* **1997**, *276*, 196.

(2) (a) Nah, M.-K.; Cho, H.-G.; Kwon, H.-J.; Kim, Y.-J.; Park, C.; Kim, H. K.; Kang, J.-G. *J. Phys. Chem. A* **2006**, *110*, 10371. (b) Kim, H. K.; Oh, J. B.; Baek, N. S.; Roh, S.-G.; Nah, M.-K.; Kim, Y. H. *Bull. Korean Chem. Soc.* **2005**, *26*, 201. (c) Klink, S. I.; Grave, L,; Reinhoudt, D. N.; van Veggel, F. C. J. M.; Werts, M. H. V.; Geurts, F. A. J.; Hofstraat, J. W. *J. Phys. Chem. A* **2000**, *104*, 5457.

(3) (a) Oh, J. B.; Kim, Y. H.; Nah, M.-K.; Kim, H. K. *J. Luminescence* **2005**, *111*, 255. (b) Foley, T. J.; Harrison, B. S.; Knefely, A. S.; Abboud, K. A.; Reynolds, J. R.; Schanze, K. S.; Boncella, J. M. *Inorg. Chem.* **2003**, *42*, 5023. (c) Hiroshi. T.; Satoshi, S. *Chem. Rev.* **2002**, *102*, 2389.

(4) (a) Paik, K. L.; Kim, H. K. *Mol. Cryst. Liq. Cryst.* **2001**, *370*, 185. (b) Oh, J. B,; Nah, M.-K.; Kim, Y. H.; Kang, M. S.; Kim, H. K. *Adv. Funct. Mater.*, in press.

(5) (a) Gonçalves e Silva, F. R.; Malta. O. L.; Reinhard, C.; Güdel, H.-U.; Piguet, C.; Moser, J. E.; Bünzli, J.-C. G. *J. Phys. Chem. A* **2002**,

106, 1670. (b) de Sá, G. F.; Malta, O. L.; de Mello Donegá, C.; Simas, A. M.; Longo, R. L.; Santa-Cruz, P. A.; da Silva, E. F., Jr. *Coord. Chem. Rev.* **2000**, *196*, 165. (c) Malta, O. L.; Gonçalves e Silva, F. R. *Spectrochim. Acta, Part A* **1998**, *54*, 1593. (d) Malta, O. L. *J. Luminescence* **1997**, *71*, 229. (e) Faucher, M.; Malta, O. *Rare Earths Mod. Sci. Technol.* **1982**, *3*, 115.

(6) (a) Ha, J.-H.; Ko, S.; Lee, C.-H.; Lee, W.-Y.; Kim, Y.-R. *Chem. Phys. Lett.* **2001**, *349*, 271. (b) Bensasson, R.; Land, E. J. *Photochem. Photobiol. Rev.* **1978**, *3*, 163. (c) Angeli, N. G.; Lagorio, M. G.; San Román, E. A.; Dicelio, L. E. *Photochem. Photobiol.* **2000**, *72*, 49.

(7) Demas, J. N.; Crosby, G. A. *J. Phys. Chem.* **1971**, *75*, 991.

(8) Kushida, T. *J. Phys. Soc. Japan* **1973**, *34*, 1318, 1327 and 1334.

(9) Carnall, W. T.; Fields, P. R.; Rajnak, K. *J. Chem. Phys.* **1968**, *49*, 4424.

(10) Lakovicz, J. R. *Principles of Fluorescence Spectroscopy*, 2nd ed.; Kluwer Academic/ Plenum Publishers: New York, 1999.

(11) Muror, S. L.; Carmichael, I.; Hug, G. L. *Handbook of Photochemistry*, 2nd. ed.; Marcel Dekker Inc.: New York, 1993.

(12) Stein, G.; Würzberg, E. *J. Chem. Phys.* **1975**, *62*, 208.

(13) Weber, M. *J. Phys. Rev.* **1968**, *171*, 283.

(14) (a) Li, Y.; Yang, H.; He, Z.; Liu, L.; Wang, W.; Li, F.; Xu, L. *J. Mater. Res.* **2005**, *20*, 2940. (b) Pizzoferrato, R.; Lagonigro, L.; Ziller, T.; Di Carlo, A.; Paolesse, R.; Mandoj, F.; Ricci, A.; Lo Sterzo, C. *Chem. Phys.* **2004**, *300*, 217.

(15) Angelov, B. M. *J. Phys. C* **1984**, *17*, 1709.

(16) Faucher, M.; Garcia, D. *Phys. Rev. B* **1982**, *26*, 5451.

(17) Devin, M. T.; Stephens, E. M.; Richardson, F. S.; van Cott, T. C.; Davis, S. A. *Inorg. Chem.* **1987**, *26*, 1204.

(18) Kalyansundaram, K. *Photochemistry of Polypyridine and Porphyrin Complexes*; Academic Press Inc./Harcourt Brace Jovanovich: San Diego, CA, 1992.